

Article

# Geometry of chalcogenide negative curvature fibers for CO<sub>2</sub> laser transmission

Chengli Wei<sup>1</sup> , Curtis R. Menyuk<sup>2</sup>  and Jonathan Hu<sup>1,\*</sup> 

<sup>1</sup> Department of Electrical and Computer Engineering, Baylor University, 76798 Waco, USA; jonathan\_hu@baylor.edu

<sup>2</sup> Department of Computer Science and Electrical Engineering, University of Maryland Baltimore County, 21227 Baltimore, USA; menyuk@umbc.edu

\* Correspondence: jonathan\_hu@baylor.edu; Tel.: +1-254-710-1853

**Abstract:** We study impact of geometry on leakage loss in negative curvature fibers made with As<sub>2</sub>Se<sub>3</sub> chalcogenide and As<sub>2</sub>S<sub>3</sub> chalcogenide glasses for carbon dioxide (CO<sub>2</sub>) laser transmission. The minimum leakage loss decreases when the core diameter increases both for fibers with six and for fibers with eight cladding tubes. The optimum gap corresponding to the minimum loss increases when the core diameter increases for negative curvature fibers with six cladding tubes. For negative curvature fibers with eight cladding tubes, the optimum gap is always less than 20 μm when the core diameter ranges from 300 μm to 500 μm. The influence of material loss on fiber loss is also studied. When material loss exceeds 10<sup>2</sup> dB/m, it dominates the fiber leakage loss for negative curvature fiber at a wavelength of 10.6 μm.

**Keywords:** CO<sub>2</sub> lasers; negative curvature fibers; chalcogenide glass; fiber loss; mid-IR

## 1. Introduction

Carbon dioxide (CO<sub>2</sub>) lasers have been widely used in surgery, medicine, and material processing [1–3]. Step index fibers are commonly used to transmit CO<sub>2</sub> laser light. The nonlinearity in the silica glass limits the transmitted power. Hollow-core fibers have low nonlinearity, because the light is mostly transmitted in air, which does not contribute to the nonlinearity. In addition, it is possible in principle to obtain a lower loss in hollow-core fiber than in step-index fiber because air does not contribute to material loss [4,5]. Recently, hollow-core negative curvature fibers have drawn a large amount of attention due to their attractive properties including low loss, broad bandwidth, and a high damage threshold [6–12]. The delivery of mid-infrared radiation has also been successfully demonstrated using chalcogenide negative curvature fibers for a CO<sub>2</sub> laser at a wavelength of 10.6 μm [13–15]. Previous study shows that chalcogenide glass should be used for wavelength larger than 4.5 μm [16]. The relative simplicity of the negative curvature structure could enable the fabrication of fiber devices for mid-IR applications using non-silica glasses, such as chalcogenide [13–15].

The guiding mechanism in negative curvature fibers is inhibited coupling [10,17,18]. A large amount of research [10,19] has been carried out to determine the impact of the fiber parameters on the leakage loss [20] in negative curvature fibers and then optimize these parameters to minimize the loss. These parameters include the curvature of the core boundary, the number of cladding tubes, the thickness of the tubes, and the nested cladding tubes [17,18,21–24]. By introducing a gap between cladding tubes, the loss can be decreased in negative curvature fibers [24,25]. When the tubes touch, modes exist in the localized node area. A separation between the cladding tubes removes the additional resonances due to the localized node. Fibers with a gap between tubes are also expected to be easier to fabricate, since surface tension would naturally assist to maintain the circular shape of the tubes [22]. On the other hand, when the gap is too big, the core mode can leak through the gaps, which increases the loss in negative curvature fibers [26]. Therefore, an optimum gap exists. The optimal gap corresponding to the minimum loss in a fiber with six cladding tubes is three times as large as

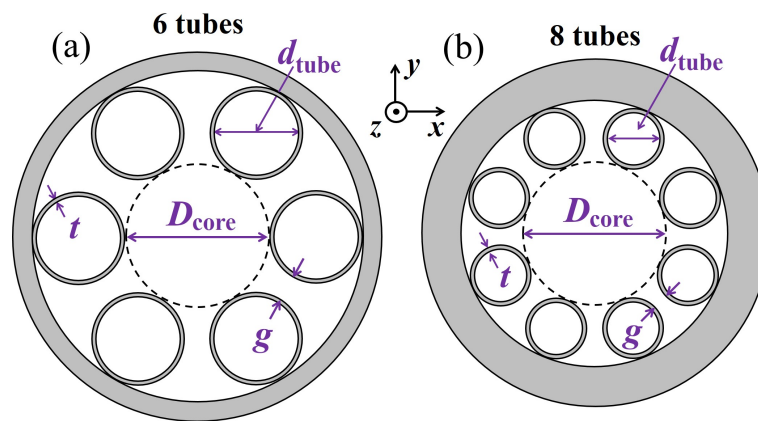


**Figure 1.** Schematic illustration of negative curvature fibers with (a) six and (b) eight cladding tubes.

36 the optimal gap in fibers with eight or ten cladding tubes [26]. A larger gap is required to remove the  
 37 weak coupling between the core mode and tube modes in a fiber with six cladding tubes [26].

38 In this paper, we find optimal structures of chalcogenide negative curvature fibers for CO<sub>2</sub> laser  
 39 transmission, in which we minimize the loss in the two-dimensional parameter space that consists  
 40 of the core diameter and the gap size. In previous studies, the optimum gap was found in negative  
 41 curvature fibers with a fixed core diameter [26]. We find that the minimum leakage loss decreases  
 42 when the core diameter increases both for fibers with six and for fibers with eight cladding tubes.  
 43 The optimum gap increases when the core diameter increases for negative curvature fibers with six  
 44 cladding tubes. The optimum gap is always less than 20 μm when the core diameter increases for  
 45 negative curvature fibers with eight cladding tubes when the core diameter ranges from 300 μm to  
 46 500 μm.

## 47 2. Geometry

48 Negative curvature fibers with six and eight cladding tubes have been fabricated by several  
 49 research groups [17,25,27,28]. Figure 1 shows schematic illustrations of negative curvature fibers with  
 50 six and eight cladding tubes. The gray regions represent glass, and the white regions represent air.  
 51 The inner tube diameter,  $d_{\text{tube}}$ , the core diameter,  $D_{\text{core}}$ , the tube wall thickness,  $t$ , the minimum gap  
 52 between the cladding tubes,  $g$ , and the number of tubes,  $p$ , are related by the expression:  $D_{\text{core}} =$   
 53  $(d_{\text{tube}} + 2t + g)\sin(\pi/p) - (d_{\text{tube}} + 2t)$  [29]. The wavelength of 10.6 μm for a CO<sub>2</sub> laser is used in our  
 54 simulation.

## 55 3. As<sub>2</sub>Se<sub>3</sub> chalcogenide glass

56 In this section, we study the loss in negative curvature fibers made with As<sub>2</sub>Se<sub>3</sub> chalcogenide  
 57 glass. The material loss of 10.6 dB/m for As<sub>2</sub>Se<sub>3</sub> chalcogenide glass is included in the simulation [30].  
 58 The tube thickness,  $t$ , is fixed at 5.2 μm corresponding to the third antiresonance. A glass thickness  
 59 corresponding to the third antiresonance has been drawn in the past [15]. We first study negative  
 60 curvature fibers with six cladding tubes. We define  $d_{6\text{max}}$  as the maximum possible tube diameter for  
 61 the fiber with 6 cladding tubes, which equals  $D_{\text{core}} - 2t$ . Figure 2(a) shows the contour plot of loss as a  
 62 function of core diameter,  $D_{\text{core}}$ , and normalized tube diameter,  $d_{\text{tube}}/d_{6\text{max}}$ . For a fixed  $D_{\text{core}}$ , the loss  
 63 decreases and then increases when  $d_{\text{tube}}/d_{6\text{max}}$  increases from 0.2 to 1.0. The minimum loss occurs  
 64 when  $d_{\text{tube}}/d_{6\text{max}} = 0.62$ , and it does not change when  $D_{\text{core}}$  increases from 300 μm to 500 μm. The loss  
 65 decreases when  $D_{\text{core}}$  increases. In addition, we show the loss as a function of the core diameter,  $D_{\text{core}}$ ,  
 66 and the gap,  $g$ , in Fig. 2(b). The loss first decreases and then increases as the gap,  $g$ , increases. When  
 67 there is no gap, a mode exists in the node that is created by the two touching tubes [25]. When the gap  
 68 is too large, core mode leaks through the gap [17,26]. We also plot the loss as a function of gap,  $g$ , for

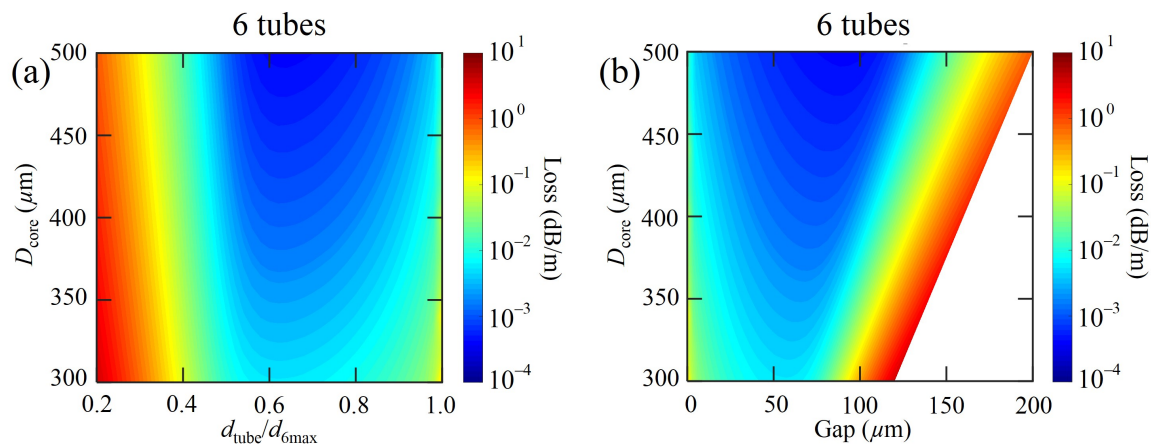


**Figure 2.** (a) Contour plot of loss as a function of core diameter and normalized tube diameter. (b) Contour plot of loss as a function of core diameter and gap. The number of cladding tube is six.

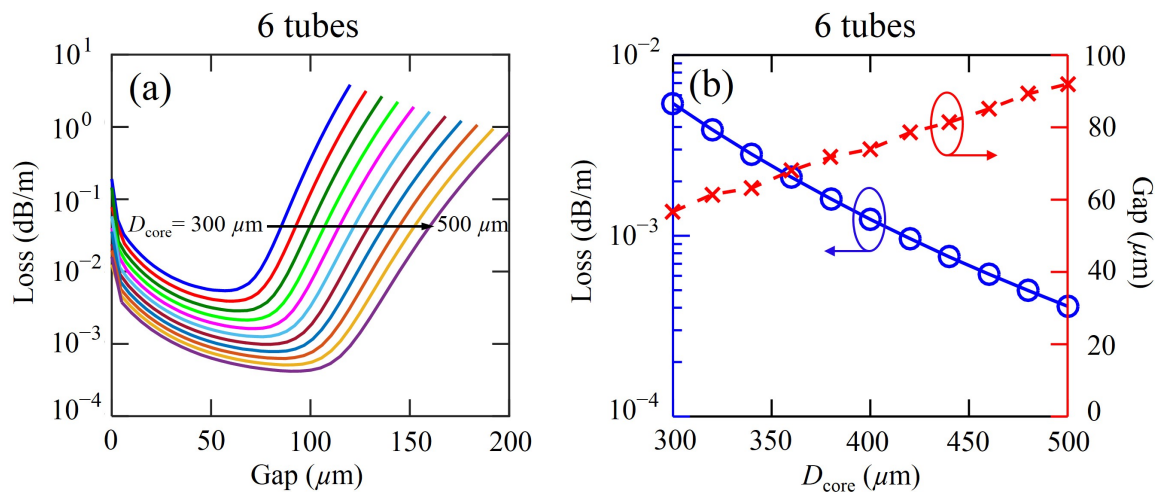


**Figure 3.** (a) Loss as a function of gap in fibers with different core diameters. (b) Minimum loss and the corresponding optimum gap in fibers with different core diameters. The number of cladding tube is six.

69 different core diameters in Fig. 3(a). In order to quantify the minimum loss and the corresponding  
 70 optimum gap for different core diameters, we also plot the minimum loss and the corresponding  
 71 optimum gap,  $g$ , using blue solid curve and red dashed curves, respectively, in Fig. 3(b). When the  
 72 core diameter increases from 300  $\mu\text{m}$  to 500  $\mu\text{m}$ , the minimum loss decreases by more than one order  
 73 of magnitude and the corresponding optimum gap,  $g$ , increases from 60  $\mu\text{m}$  to 90  $\mu\text{m}$ . Hence, a larger  
 74 gap is needed for a fiber with a larger core diameter to lower the loss in negative curvature fibers with  
 75 six cladding tubes.

76 We next carry out the same loss analysis on negative curvature fibers with eight cladding tubes.  
 77 Figure 4(a) shows the contour plot of loss as a function of core diameter,  $D_{\text{core}}$ , and normalized tube  
 78 diameter,  $d_{\text{tube}}/d_{8\text{max}}$ , where  $d_{8\text{max}}$  is defined as the maximum possible tube diameter for the fiber  
 79 with 8 cladding tubes, which is  $\{D_{\text{core}}\sin(\pi/8) - 2t[1 - \sin(\pi/8)]\}/[1 - \sin(\pi/8)]$  [31]. Figure 4(b)  
 80 shows the contour plot of loss as a function of core diameter,  $D_{\text{core}}$ , and gap,  $g$ . The minimum loss  
 81 occurs at a larger value of  $d_{\text{tube}}/d_{8\text{max}}$ , or a smaller value of  $g$ , than is the case for negative curvature  
 82 fibers with six cladding tubes. In Fig. 5(a), we show the loss as a function of the gap,  $g$ , for different

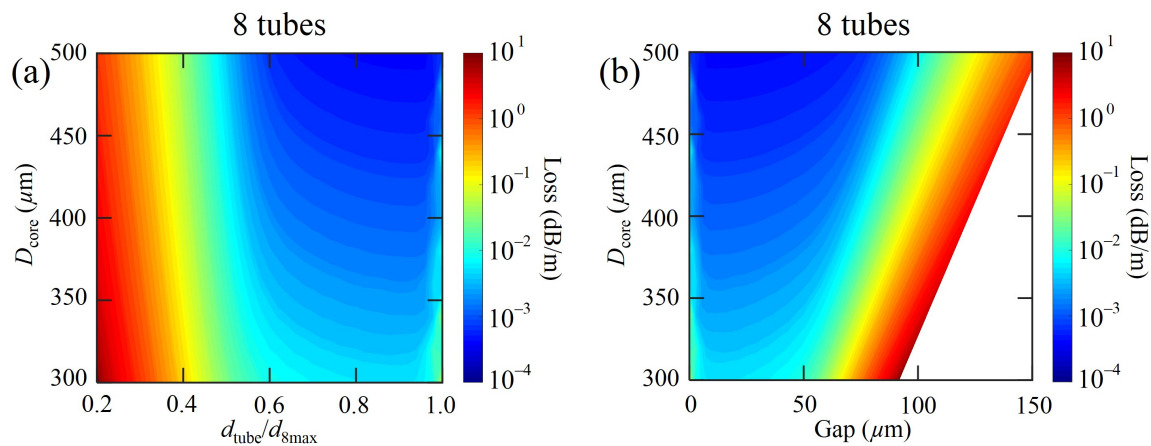


**Figure 4.** (a) Contour plot of loss as a function of core diameter and normalized tube diameter. (b) Contour plot of loss as a function of the core diameter and gap. The number of cladding tube is eight.

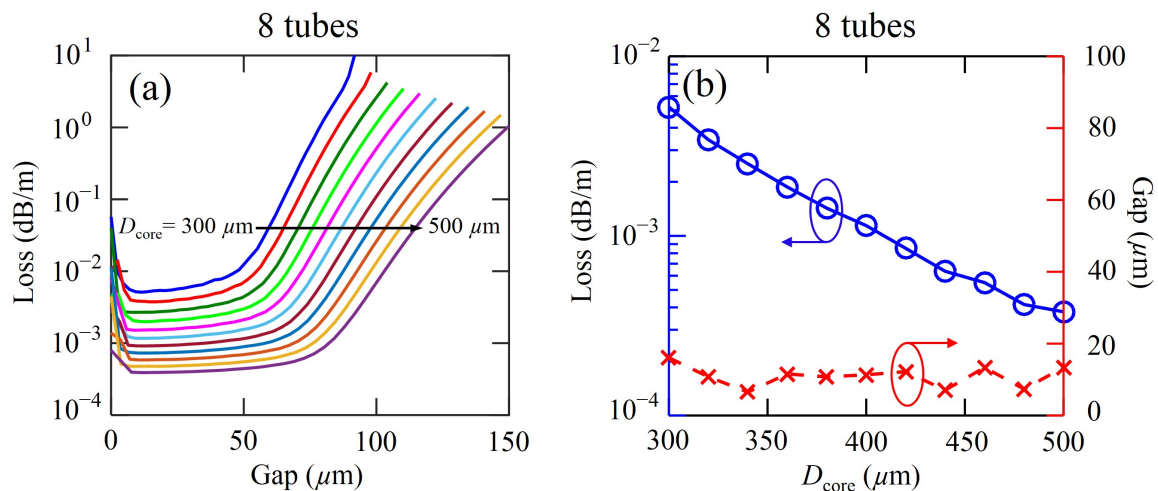


**Figure 5.** (a) Loss as a function of the gap in fibers with different core diameters. (b) Minimum loss and the corresponding gap in fibers with different core diameters. The number of cladding tubes is eight.

83 core diameters. The optimum gap corresponding to the minimum loss is less than  $20 \mu\text{m}$  for fibers with  
 84 different core diameters and the loss increases slowly when gap further increases. The minimum loss  
 85 and the corresponding gap,  $g$ , are plotted using blue solid curve and red dashed curves, respectively,  
 86 in Fig. 5(b). The minimum loss decreases by around one order of magnitude when the core diameter  
 87 increases from  $300 \mu\text{m}$  to  $500 \mu\text{m}$ . Different from fibers with six cladding tubes, the corresponding  
 88 optimum gap,  $g$ , is much smaller and is always less than  $20 \mu\text{m}$  when the core diameter increases from  
 89  $300 \mu\text{m}$  to  $500 \mu\text{m}$  in fibers with eight cladding tubes. There is a wide range of gaps that realize low  
 90 loss in the fibers with eight cladding tubes, as shown in Fig. 5(a). The loss is less sensitive to the gap in  
 91 the region between  $10 \mu\text{m}$  and  $50 \mu\text{m}$ . Since the tube diameter is much smaller than the diameter of  
 92 core, the coupling between the core mode and tube modes is weak. A larger gap is needed for fibers  
 93 with six cladding tubes to remove the weak coupling between the core mode and cladding tube modes  
 94 in negative curvature fibers with six cladding tubes.

#### 95 4. As<sub>2</sub>S<sub>3</sub> chalcogenide glass

96 In this section, we carried out the same loss analysis in negative curvature fibers made with As<sub>2</sub>S<sub>3</sub>  
 97 chalcogenide glass. The material loss of 500 dB/m for As<sub>2</sub>S<sub>3</sub> chalcogenide glass is included in the  
 98 simulation [15,16]. The tube thickness,  $t$ , is fixed at 6.1  $\mu\text{m}$  corresponding to the third antiresonance.  
 99 Figure 6(a) shows the loss as a function of gap,  $g$ , when the core diameter increases from 300  $\mu\text{m}$   
 100 to 500  $\mu\text{m}$  in As<sub>2</sub>S<sub>3</sub> chalcogenide fiber with six cladding tubes. Compared with the loss in Fig. 3(a),  
 101 the losses in the fiber using As<sub>2</sub>S<sub>3</sub> chalcogenide glass, shown in Fig. 6(a), are higher and have a flatter  
 102 minimum. In Fig. 6(b), we show the minimum loss and the corresponding gap,  $g$ , as blue solid curve  
 103 and red dashed curve, respectively. We also study the fiber leakage loss with and without material loss  
 104 in an As<sub>2</sub>S<sub>3</sub> chalcogenide fiber with six cladding tubes. In Fig. 7(a), we show the results in order to  
 105 explain the broad, low-loss region in Fig. 6(a). The core diameter is fixed at 300  $\mu\text{m}$ . The solid curve  
 106 shows the fiber loss with material loss of 500 dB/m for As<sub>2</sub>S<sub>3</sub> chalcogenide glass, which is the same as  
 107 the blue solid curve in Fig. 6(a). The dashed curve shows the fiber loss without material loss, which  
 108 is similar to the curve in Fig. 3(a). The high material loss of As<sub>2</sub>S<sub>3</sub> chalcogenide glass dominates and  
 109 leads to a flat minimum in the fiber loss curve, as shown by the blue solid curve in Fig. 7(a).

110 In order to better illustrate the influence of the material loss on the total fiber loss, we study the  
 111 fiber loss as a function of material loss both for As<sub>2</sub>S<sub>3</sub> chalcogenide glass and As<sub>2</sub>Se<sub>3</sub> chalcogenide  
 112 glass, shown in Fig. 7(b) as the red dashed and blue solid curves, respectively. The core diameter  
 113 is 300  $\mu\text{m}$  and the gap is 60  $\mu\text{m}$ . The fiber loss changes little when the material loss increases from  
 114 0.1 dB/m to 10 dB/m, and the fiber loss is dominated by the confinement loss in the blue region for  
 115 both curves. The loss of fiber that is made with As<sub>2</sub>Se<sub>3</sub> chalcogenide glass is located in the blue region,  
 116 which is marked with the blue circle on the blue solid curve. The fiber loss begins to increase when  
 117 the material loss increases from 10 dB/m to 10<sup>2</sup> dB/m, and the influence of the material loss becomes  
 118 visible. When the material loss further increases, the fiber loss increases sharply, and the fiber loss is  
 119 dominated by the material loss in the red region for both curves, when the material loss is higher than  
 120 10<sup>2</sup> dB/m. The loss of fiber made with As<sub>2</sub>S<sub>3</sub> chalcogenide glass is located in the red region, which  
 121 is marked with the red triangle on the red dashed curve.

122 Figure 8(a) shows the loss as a function of gap,  $g$ , in As<sub>2</sub>S<sub>3</sub> chalcogenide fiber with eight cladding  
 123 tubes. In Fig. 8(b), we show the minimum loss and the corresponding gap,  $g$ , using a blue solid curve  
 124 and a red dashed curve, respectively. The minimum loss decreases by less than one order of magnitude  
 125 and the corresponding optimum gap,  $g$ , is always less than 20  $\mu\text{m}$ , which agrees with the results in the

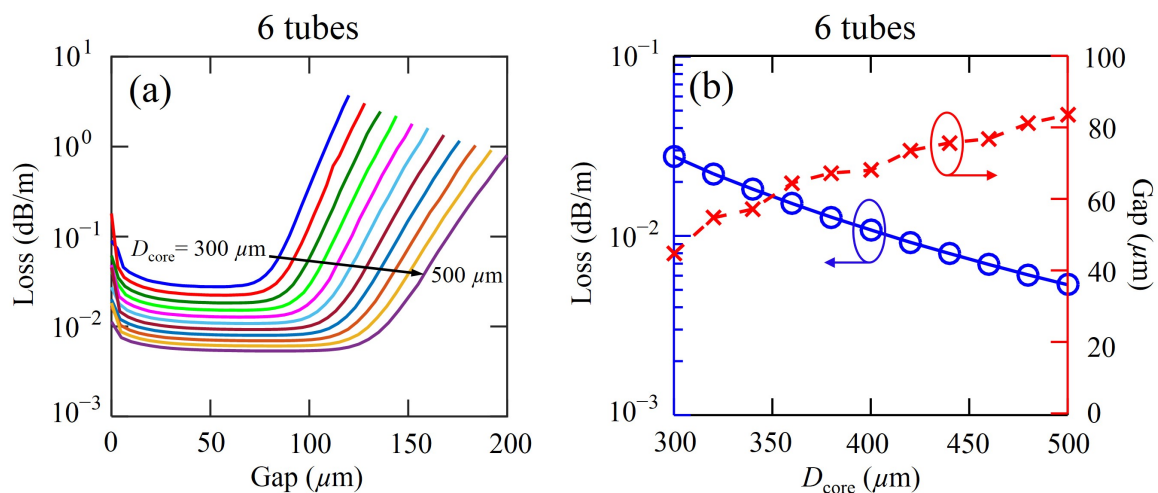


**Figure 6.** (a) Loss as a function of gap in fibers with different core diameters. (b) Minimum loss and corresponding optimum gap in fibers with different core diameters. There are six cladding tubes.

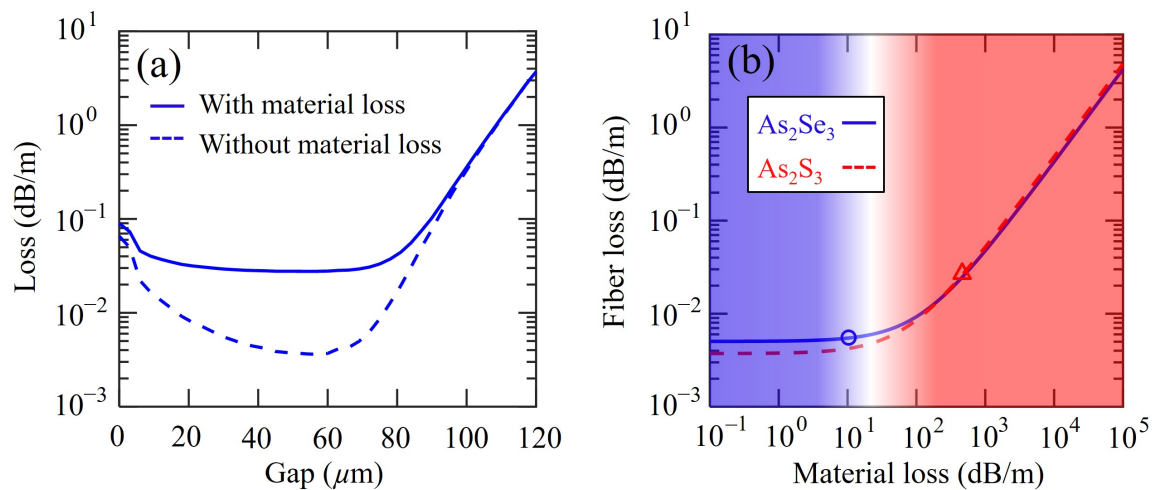


**Figure 7.** (a) Loss as a function of gap in fibers with and without material loss. (b) Fiber loss as a function of material loss in  $\text{As}_2\text{Se}_3$  chalcogenide glass fiber and  $\text{As}_2\text{S}_3$  chalcogenide glass fiber with six cladding tubes, a core diameter of  $300 \mu\text{m}$ , and a gap of  $60 \mu\text{m}$ .

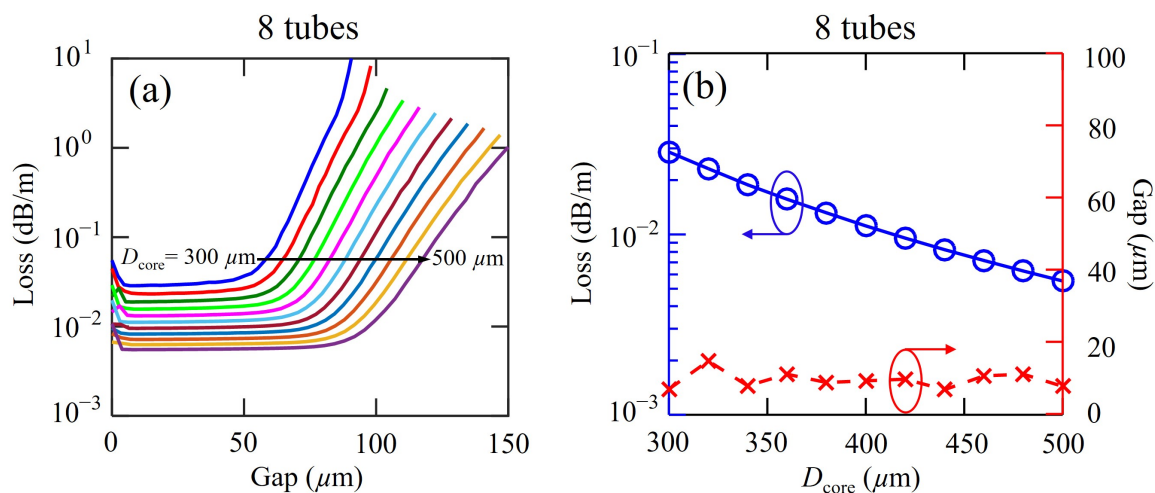


**Figure 8.** (a) Loss as a function of gap in fibers with different core diameters. (b) Minimum loss and corresponding gap in fibers with different core diameters. The number of cladding tube is eight.

126  $\text{As}_2\text{Se}_3$  chalcogenide fiber with 8 cladding tubes. Small loss variation near zero gap occurs due to the  
 127 glass modes existed near the node area between two tubes in Fig. 8(a).

## 128 5. Conclusions

129 In this paper, we optimize the structure of negative curvature fibers for  $\text{CO}_2$  laser transmission. We  
 130 investigate the impact of the size of the gap between cladding tubes on the loss of negative curvature  
 131 fibers made with  $\text{As}_2\text{Se}_3$  and  $\text{As}_2\text{S}_3$  chalcogenide glasses. For  $\text{As}_2\text{Se}_3$  chalcogenide fibers with six  
 132 cladding tubes, the minimum loss decreases by an order of magnitude and the corresponding optimum  
 133 gap,  $g$ , increases from  $60 \mu\text{m}$  to  $90 \mu\text{m}$  when the core diameter increases from  $300 \mu\text{m}$  to  $500 \mu\text{m}$ . A  
 134 greater gap is needed for a fiber with greater core diameter to reduce the coupling between the core  
 135 mode and tube mode. For a fiber with eight cladding tubes, the optimum gap,  $g$ , that corresponds to  
 136 the minimum loss is always less than  $20 \mu\text{m}$  when the core diameter ranges from  $300 \mu\text{m}$  to  $500 \mu\text{m}$ . We  
 137 also study  $\text{As}_2\text{S}_3$  chalcogenide fibers, which has a higher material loss at a wavelength of  $10.6 \mu\text{m}$ . It is

138 found that material loss dominates the fiber leakage loss. The fiber loss is dominated by the material  
139 loss, when the material absorption loss is higher than  $10^2$  dB/m.

140 **Author Contributions:** Supervision, Curtis Menyuk and Jonathan Hu; Validation, Curtis Menyuk and Jonathan  
141 Hu; Writing – original draft, Chengli Wei; Writing – review & editing, Chengli Wei, Curtis Menyuk and Jonathan  
142 Hu.

143 **Conflicts of Interest:** The authors declare no conflict of interest.

## 144 References

- 145 1. Snakenborg, D.; Klank, H.; Kutter, J. P. Microstructure fabrication with a CO<sub>2</sub> laser system. *J. Micromech.*  
146 *Microeng.* **2004**, *14*, 182–189.
- 147 2. Hædersdal, M.; Sakamoto, F.H.; Farinelli, W.A.; Doukas, A.G.; Tam, J.; Anderson, R.R. Fractional CO<sub>2</sub>  
148 laser-assisted drug delivery. *Lasers Surg. Med.* **2010**, *42*, 113–122.
- 149 3. Witteman, W.J. In *The CO<sub>2</sub> Laser*; Enoch, J.F., Macadam, D.L., Schawlow, A.L., Shimoda, K., Tamir, T.;  
150 Springer-Verlag: Berlin, Germany, 1987; pp. 1–4, ISBN 978-3-540-47744-0.
- 151 4. Poletti, F.; Petrovich, M.N.; Richardson, D. J. Hollow-core photonic bandgap fibers: technology and  
152 applications. *Nanophotonics* **2013**, *2*, 315–340.
- 153 5. Roberts, P.J.; Couny, F.; Sabert, H.; Mangan, B.J.; Williams, D.P.; Farr, L.; Mason, M.W.; Tomlinson, A.; Birks,  
154 T.A.; Knight, J.C.; Russell, P.St.J. Ultimate low loss of hollow-core photonic crystal fibres. *Opt. Express* **2005**,  
155 *13*, 236–244 .
- 156 6. Wang, Y.; Couny, F.; Roberts, P.J.; Benabid, F. Low loss broadband transmission in optimized core-shaped  
157 Kagome hollow-core PCF. In Proceedings of the Lasers Electro-Optics, Quantum Electron, Laser Science  
158 Conference, San Jose, CA, USA, 16–21 May 2010; paper CPDB4.
- 159 7. Wang, Y.Y.; Wheeler, N.V.; Couny, F.; Roberts, P.J.; Benabid, F. Low loss broadband transmission in  
160 hypocycloid-core Kagome hollow-core photonic crystal fiber. *Opt. Lett.* **2011**, *36*, 669–671.
- 161 8. Pryamikov, A.D.; Biriukov, A.S.; Kosolapov, A.F.; Plotnichenko, V.G.; Semjonov, S.L.; Dianov, E. M.  
162 Demonstration of a waveguide regime for a silica hollow-core microstructured optical fiber with a negative  
163 curvature of the core boundary in the spectral region  $>3.5$   $\mu\text{m}$ . *Opt. Express* **2011**, *19*, 1441–1448 .
- 164 9. Yu, F.; Wadsworth, W. J.; Knight, J. C. Low loss silica hollow core fibers for 3–4  $\mu\text{m}$  spectral region. *Opt.*  
165 *Express* **2012**, *20*, 11153–11158.
- 166 10. Wei, C.; Weiblen, R. J.; Menyuk, C. R.; Hu, J. Negative curvature fibers. *Adv. Opt. Photon.* **2017**, *9*, 504–561.
- 167 11. Michieletto, M.; Lyngs, J.K.; Jakobsen, C.; Lsggaard, J.; Bang, O.; Alkeskjold, T.T. Hollow-core fibers for high  
168 power pulse delivery. *Opt. Express* **2016**, *24*, 7103–7119.
- 169 12. Wei, C.; Menyuk, C. R.; Hu, J. Polarization-filtering and polarization-maintaining low-loss negative curvature  
170 fibers. *Opt. Express* **2018**, *26*, 9528–9540.
- 171 13. Kosolapov, A.F.; Pryamikov, A.D.; Biriukov, A.S.; Shiryayev, V.S.; Astapovich, M.S.; Snopatin, G.E.;  
172 Plotnichenko, V.G.; Churbanov, M.F.; Dianov, E.M. Demonstration of CO<sub>2</sub>-laser power delivery through  
173 chalcogenide glass fiber with negative-curvature hollow core. *Opt. Express* **2011**, *19*, 2572–25728.
- 174 14. Shiryayev, V.S. Chalcogenide glass hollow-core microstructured optical fibers. *Front. Mater.* **2015**, *2*, 24.
- 175 15. Gattass, R.R.; Rhonehouse, D.; Gibson, D.; McClain, C.C.; Thapa, R.; Nguyen, V.Q.; Bayya, S.S.; Weiblen,  
176 R.J.; Menyuk, C.R.; Shaw, L.B.; Sanghera, J.S. Infrared glass-based negative-curvature anti-resonant fibers  
177 fabricated through extrusion. *Opt. Express* **2016**, *14*, 25697–25703 .
- 178 16. Wei, C.; Hu, J.; Menyuk, C.R. Comparison of loss in silica and chalcogenide negative curvature fibers as the  
179 wavelength varies. *Front. Phys.* **2016**, *4*, 30.
- 180 17. Debord, B.; Amsanpally, A.; Chafer, M.; Baz, A.; Maurel, M.; Blondy, J. M.; Hugonnot, E.; Scol, F.; Vincetti, L.;  
181 G r me, F.; Benabid, F. Ultralow transmission loss in inhibited-coupling guiding hollow fibers. *Optica* **2017**,  
182 *4*, 209–217 .
- 183 18. Debord, B.; Alharbi, M.; Bradley, T.; Fourcade-Dutin, C.; Wang, Y.Y.; Vincetti, L.; G r m, F.; Benabid, F.  
184 Hypocycloid-shaped hollow-core photonic crystal fiber Part I: arc curvature effect on confinement loss. *Opt.*  
185 *Express* **2013**, *21*, 28597–28608.
- 186 19. Yu, F.; Knight, J. C. Negative curvature hollow-core optical fiber. *IEEE J. Sel. Top. Quantum Electron.* **2016**, *22*,  
187 4400610.

- 188 20. Hu, J.; Menyuk, C. R. Understanding leaky modes: slab waveguide revisited. *Adv. Opt. Photon.* **2009**, *1*,  
189 58–106.
- 190 21. Alagashev, G.K.; Pryamikov, A.D.; Kosolapov, A.F.; Kolyadin, A.N.; Lukovkin, A.Y.; Biriukov, A.S. Impact of  
191 geometrical parameters on the optical properties of negative curvature hollow core fibers. *Laser Phys.* **2015**,  
192 *25*, 055101.
- 193 22. Poletti, F. Nested antiresonant nodeless hollow core fiber. *Opt. Express* **2014**, *22*, 23807–23828.
- 194 23. Habib, M.S.; Bang, O.; Bache, M. Low-loss hollow-core silica fibers with adjacent nested anti-resonant tubes.  
195 *Opt. Express* **2015**, *23*, 17394–17406.
- 196 24. Belardi, W.; Knight, J. C. Hollow antiresonant fibers with reduced attenuation. *Opt. Lett.* **2014**, *39*, 1853–1856.
- 197 25. Kolyadin, A.N.; Kosolapov, A.F.; Pryamikov, A.D.; Biriukov, A.S.; Plotnichenko, V.G.; Dianov, E.M. Light  
198 transmission in negative curvature hollow core fiber in extremely high material loss region. *Opt. Express*  
199 **2013**, *21*, 9514–9519.
- 200 26. Wei, C.; Menyuk, C.R.; Hu, J. Impact of cladding tubes in chalcogenide negative curvature fibers. *IEEE*  
201 *Photon. J.* **2016**, *8*, 2200509.
- 202 27. Uebel, P.; Günendi, M. C.; Frosz, M.H.; Ahmed, G.; Edavalath, N. N.; Ménard, J.-M.; Russell, P. St.J.  
203 Broadband robustly single-mode hollow-core PCF by resonant filtering of higher-order modes. *Opt. Lett.*  
204 **2016**, *41*, 1961–1964.
- 205 28. Liu, X.; Ding, W.; Wang, Y. Y.; Gao, S.; Cao, L.; Feng, X.; Wang, P. Characterization of a liquid-filled nodeless  
206 anti-resonant fiber for biochemical sensing. *Opt. Lett.* **2017**, *42*, 863–866.
- 207 29. Wei, C.; Menyuk, C.R.; Hu, J. Bending-induced mode non-degeneracy and coupling in chalcogenide negative  
208 curvature fibers. *Opt. Express* **2016**, *24*, 12228–12239.
- 209 30. Caillaud, C.; Renversez, G.; Brilland, L.; Mechin, D.; Calvez, L.; Adam, J.-L.; Troles, J. Photonic Bandgap  
210 Propagation in All-Solid Chalcogenide Microstructured Optical Fibers. *Materials* **2014**, *7*, 6120–6129.
- 211 31. Wei, C.; Kuis, R.A.; Chenard, F.; Menyuk, C.R.; Hu, J. Higher-order mode suppression in chalcogenide  
212 negative curvature fibers. *Opt. Express* **2015**, *23*, 15824–15832.